Intermittent stimulus presentation stabilizes neuronal responses in macaque area MT

P. Christiaan Klink, Anna Oleksiak, Martin J. M. Lankheet and Richard J. A. van Wezel

J Neurophysiol 108:2101-2114, 2012. First published 25 July 2012;
doi: 10.1152/jn.00252.2012

J Neurophysiol 108: 2101–2114, 2012.
First published July 25, 2012; doi:10.1152/jn.00252.2012.

Intermittent stimulus presentation stabilizes neuronal responses in macaque area MT

P. Christiaan Klink,[1,2] Anna Oleksiak,[1,2] Martin J. M. Lankheet,[3] and Richard J. A. van Wezel[1,2,4,5]

[1]*Functional Neurobiology, Helmholtz Institute, Utrecht University, Utrecht, The Netherlands;* [2]*Division of Pharmacology, Utrecht Institute for Pharmaceutical Sciences, Utrecht University, Utrecht, The Netherlands;* [3]*Experimental Zoology, Wageningen University, Wageningen, The Netherlands;* [4]*Biomedical Signals and Systems, MIRA, Twente University, Enschede, The Netherlands; and* [5]*Department of Biophysics, Donders Institute for Brain, Cognition and Behaviour, Radboud University, Nijmegen, The Netherlands*

Submitted 23 March 2012; accepted in final form 24 July 2012

Klink PC, Oleksiak A, Lankheet MJ, van Wezel RJ. Intermittent stimulus presentation stabilizes neuronal responses in macaque area MT. *J Neurophysiol* 108: 2101–2114, 2012. First published July 25, 2012; doi:10.1152/jn.00252.2012.—Repeated stimulation impacts neuronal responses. Here we show how response characteristics of sensory neurons in macaque visual cortex are influenced by the duration of the interruptions during intermittent stimulus presentation. Besides effects on response magnitude consistent with neuronal adaptation, the response variability was also systematically influenced. Spike rate variability in motion-sensitive area MT decreased when interruption durations were systematically increased from 250 to 2,000 ms. Activity fluctuations between subsequent trials and Fano factors over full response sequences were both lower with longer interruptions, while spike timing patterns became more regular. These variability changes partially depended on the response magnitude, but another significant effect that was uncorrelated with adaptation-induced changes in response magnitude was also present. Reduced response variability was furthermore accompanied by changes in spike-field coherence, pointing to the possibility that reduced spiking variability results from interactions in the local cortical network. While neuronal response stabilization may be a general effect of repeated sensory stimulation, we discuss its potential link with the phenomenon of perceptual stabilization of ambiguous stimuli as a result of interrupted presentation.

ambiguous stimuli; motion; variability; visual cortex; spike-field coherence

REPETITION IS IMPORTANT for perceptual learning and memory, but it remains largely unclear how sensory neurons alter their response characteristics when they are exposed to repeated stimulation. Studies on the effects of repetition in the brain predominantly address the reduction of response magnitude known as adaptation or fatigue (Grill-Spector et al. 2006; Kohn 2007; Mayo and Sommer 2008). However, behavioral and computational studies on the conscious perception of intermittently presented ambiguous visual stimuli suggest that repeated stimulus presentations can have much more elaborate effects on neuronal response characteristics than might be initially expected from straightforward fatigue (Leopold et al. 2002; Noest et al. 2007).

Ambiguous stimuli are patterns that contain equal sensory evidence for multiple, mutually exclusive perceptual interpretations. When these patterns are viewed continuously, perception lapses into fluctuations between alternative stimulus interpretations. Temporarily removing an ambiguous pattern from view severely reduces the number of perceptual fluctuations and stabilizes perception into one of the possible stimulus interpretations (Klink et al. 2008; Kornmeier et al. 2007; Leopold et al. 2002; Orbach et al. 1966; Pearson and Brascamp 2008). This phenomenon is dubbed perceptual stabilization or perceptual memory, and it has been demonstrated with various distinct ambiguous patterns (Klink et al. 2008; Pearson and Brascamp 2008) even when several different patterns are presented in interleaved sequences (Maier et al. 2003).

The occurrence and depth of perceptual stabilization crucially depend on the duration for which a stimulus is removed from view (Klink et al. 2008). Long interruptions ($>$1.0 s) stabilize perceptual sequences to a single interpretation, whereas short interruptions ($<$0.5 s) destabilize perception and cause increases in the frequency of perceptual alternations. Perceptual stabilization may be related to increased neuronal responsiveness and/or to reduced neuronal response variability. Whereas stimulus presentation duration and repetition are known to affect neuronal adaptation and fatigue, it is currently unknown how the duration of temporary stimulus removal influences the neuronal response to repeated stimuli. Here we recorded spikes and local field potentials (LFPs) from neurons in motion-sensitive visual area MT of two macaque monkeys while they viewed intermittently presented visual motion stimuli that were removed from view for durations that varied between 250 and 2,000 ms.

If MT neurons take part in encoding the subjective percepts of ambiguous structure-from-motion (SFM) stimuli (Bradley et al. 1998; Parker 2007) and periodically removing such stimuli from view stabilizes perception into one specific interpretation (Klink et al. 2008; Leopold et al. 2002), then response patterns might be hypothesized to "stabilize" under these circumstances as well. A recent analysis of response variability dynamics in multiple cortical areas, including MT, demonstrated that stimulus onset consistently reduces across-trial variability, implying that cortical circuits become more stable when driven (Churchland et al. 2010). Response variability also decreases when stimuli are actively attended (Mitchell et al. 2007) or when natural stimuli are presented repeatedly (Yao et al. 2007). Building upon these findings, we hypothesize that the depth of perceptual stabilization may reflect a general, time-limited neuronal response stabilization effect that

Address for reprint requests and other correspondence: P. C. Klink, Depts. of Neuromodulation & Behaviour/Vision & Cognition, Netherlands Institute for Neuroscience, Royal Netherlands Academy of Arts and Sciences. Meibergdreef 47, 1105 BA Amsterdam, The Netherlands (e-mail: p.c.klink@gmail.com).

is promoted by an increased involvement of the local cortical circuits. On a neuronal basis, such a mechanism could manifest itself in a decrease of across-trial response variability.

MATERIALS AND METHODS

Responses were obtained from 94 neurons in two adult male rhesus macaques (*Macaca mulatta*; 46 and 48 cells, respectively) weighing 8–12 kg. Before the experiments, both monkeys were surgically implanted with a head-holding device and stainless steel recording chamber (Crist Instruments, Hagerstown, MD) that provided access to area MT. Monkeys were trained to sit in a custom-made primate chair with their head fixed and maintain their gaze within a 2°-diameter virtual fixation window surrounding a white rectangular spot (0.5° × 0.5°, 102 cd/m^2) on the screen that was located at a distance of 65.0 cm from the eyes. Upon successful fixation, the fixation spot turned red (19 cd/m^2) and stimulus presentation commenced. The monkey was periodically (every few seconds, similar for all blocks) rewarded with liquid drops for maintaining fixation. Eye positions were continuously recorded with an infrared video eye tracker sampling at 500 Hz (EyeLink; SR Research, Osgoode, ON, Canada). Whenever the monkey broke fixation, stimulus presentation stopped and the continuous fixation timer on which reward delivery was based was reset. All surgical and experimental procedures complied with Dutch and European laws and guidelines and were approved by the Utrecht University Animal Experiments Review Committee. Appropriate measures were taken to minimize pain and discomfort for the animals.

Electrophysiology. For each recording session, a Parylene-insulated tungsten microelectrode (0.1- to 2.0-MΩ impedance) was manually inserted through a stainless steel guide tube that passed the dura. This electrode was then slowly advanced with a hydraulic micropositioner (David Kopf Instruments, Tujunga, CA). Area MT was identified by the recording position and depth, the transitions between gray matter, white matter, and sulci, and the functional properties of neurons encountered along the electrode track. The extracellularly recorded signal was preamplified 1,000 times (Bak Electronics, Germantown, MD), and 50-Hz noise was removed with an adaptive filter (HumBug, Quest Scientific). The raw signal was then split into two streams, one of which was sampled and saved at 4 kHz with a CED 1401 data acquisition system together with Spike2 software (Cambridge Electronic Design) to allow off-line analysis of the LFP trace. The other stream was band-pass filtered (with a Krohn-Hite 3362 filter) between 0.1 and 2.0 kHz, after which action potentials from single neurons were detected with a window discriminator (Bak Electronics). Spike times were collected at a 2-kHz resolution with a Macintosh G4 computer equipped with a National Instruments PCI-1200 data acquisition board.

When an MT neuron was isolated, direction selectivity was initially assessed with a contralaterally presented wide-field motion stimulus comprised of high-density white dots that were coherently moving against a black background in eight different, pseudorandomly alternating directions. The size and location of the neuron's receptive field were then mapped by manually moving a bar of light across the visual field. Finally, the precise direction tuning and preferred speed of the neuron were determined by presenting additional moving dot patterns within the determined receptive field.

Visual stimuli. Stimuli were generated with custom-written software on a Macintosh G4 computer and presented on a 21-in. monitor running at a resolution of 1,024 × 768 pixels and a refresh rate of 100 Hz. All stimuli consisted of 200 white dots (102 cd/m^2) presented on a black background (~0.01 cd/m^2). The individual dot size was 0.2° × 0.2°, and the entire stimulus size was 6.7° × 6.7°. Stimuli were displayed in blocks that contained sequences of up to 120 stimulus presentations (trials) that each lasted 500 ms. The duration of the off-period between stimulus presentations was fixed within a block of presentations and pseudorandomly chosen from four possible durations (250, 500, 1,000 or 2,000 ms; Fig. 1*A*). Maintaining roughly the same number of stimulus presentations within a block while varying the intermittent blank intervals has the advantage of keeping the total amount of stimulation that a neuron receives in blocks of stimulus presentations with different blank durations approximately constant. This, however, comes at the cost of having longer blocks (in seconds) with increasing blank durations. We checked the possible confounding effects of different block durations and did not find any (see *Control for block and fixation duration* and RESULTS).

For the ambiguous SFM cylinder stimulus, dots were randomly positioned at each stimulus onset to mimic the two-dimensional projection of a three-dimensional transparent cylinder. During the 500 ms that this cylinder was presented, the dots coherently moved with an unlimited dot lifetime simulating a rotating cylinder. The speed of the simulated rotation was chosen to match the neuron's preferred speed, and the axis of rotation was orthogonal to the neuron's preferred and null directions, causing one half of the dots to move in the preferred direction and the other half in the null direction. To avoid confounding effects of attention (Klink et al. 2008; Kornmeier et al. 2009; Mitchell et al. 2004), flash suppression (Sengpiel et al. 1995; Sheinberg and Logothetis 1997; Wolfe 1984), or flash facilitation (Brascamp et al. 2007), we did not include disambiguated stimuli in the sequences of ambiguous stimuli or ask the monkeys to report their percepts. While this approach has the disadvantage of not knowing which percept corresponds to which neural trace, we believe that reducing the confounding influence of attention allows a cleaner investigation of the neuronal consequences of long sequences of stimulus presentations with different removal period durations. The two secondary stimuli were *1*) a dynamic random dot pattern (coherence 0%) for which all dots had a single frame dot lifetime and a randomized starting position on every presentation and *2*) an opaque SFM cylinder that was similar to the primary ambiguous cylinder, but here only the 100 dots that moved in the neuron's preferred direction were presented on the screen.

Data analysis. Both the raw LFP trace and the spike times were exported to MATLAB (The MathWorks, Natick, MA) for further analysis. Only responses to stimulus presentations that were part of an uninterrupted sequence (no breaks in fixation) of at least three subsequent stimulus presentations were included in further analyses. Peristimulus time histograms (PSTHs) of the spiking activity were calculated with a bin width of 10 ms, aligned to each stimulus onset. For calculations of average activities, we assumed a fixed 50-ms response latency and defined the neuronal response to the stimulus as the activity in a 500-ms time window after the 50-ms latency. The first 200-ms period of this response window was defined as the transient phase of the response, while the remaining 300-ms period was defined as the sustained phase of the response (Fig. 1*B*, *inset*, *top*).

Raw Fano factors (FFs) were obtained per cell for every combination of stimulus and off-duration by dividing the mean spike count over individual stimulus responses by the variance over these same responses in a 70-ms sliding window moving with 10-ms increments (1 PSTH bin). Additionally, we also calculated FFs by computing a linear regression between the mean spike count and the spike count variance of all cells for each sliding window position (Churchland et al. 2010). The slope of this regression analysis provides an alternative estimate of the variance to mean ratio. Such regression analysis was also performed on a randomly picked subset of the cells that had an equal overall mean spike count for all off-durations within one of the stimulus types. The "mean-matched" FF (Churchland et al. 2010) obtained from such a subset of the data is strongly resistant to FF changes that are primarily driven by variations in the mean spike count rather than in variability. While some quantitative differences in FF dynamics were observed between these three different analyses, the qualitative pattern was highly consistent. We therefore report only the results from the first-mentioned, cell-based, FF determination.

The spiking activity in the 100 ms preceding stimulus presentation was compared with the activity in the period between 50 and 150 ms

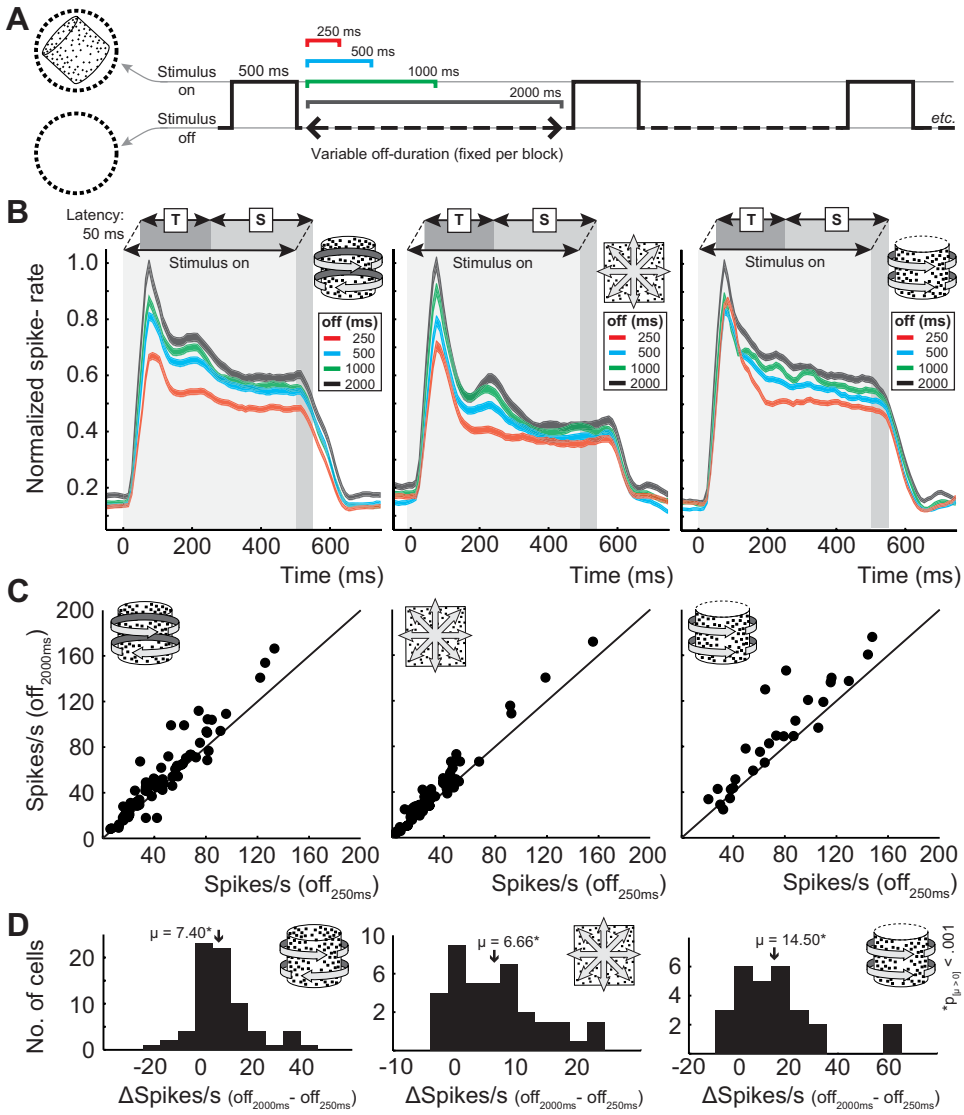

Fig. 1. Experimental paradigm and averaged response patterns. *A*: stimuli were placed in a neuron's receptive field (dotted circle) and intermittently presented with a fixed "stimulus on" period of 500 ms and a variable "stimulus off" period that was varied over blocks between 250, 500, 1,000, and 2,000 ms. *B*: averaged peristimulus time histograms for different stimuli (panels) and off-durations (colors). Histograms were calculated in 10-ms bins aligned to stimulus onset and averaged over all trials with the same combination of stimulus and off-duration (n_{amb_cyl} = 7,662, 7,244, 7,001, 4,741; n_{dyn_noi} = 4,712, 5,033, 4,557, 3,644; n_{op_cyl} = 2,263, 2,183, 1,976, 1,830 for the 4 off-durations in increasing order, respectively). For plotting purposes, the histograms were normalized to the peak value at the longest off-duration of 2,000 ms and smoothed with a 50-ms moving average window. Line thickness indicates the average value ± SE. Gray rectangular areas indicate the time range of stimulus presentation. The response, defined as the activity in a 500-ms window with a 50-ms latency relative to stimulus onset, was subdivided into a 200-ms initial transient response (marked "T") and a remaining 300-ms sustained response (marked "S"). *C*: average spike rates during full stimulus presentations for the shortest vs. the longest off-duration split up by stimulus type (panels). Dots are individual cells. *D*: distributions of differences in the average spike rates during stimulus presentation with longest and shortest off-duration over all cells. Mean differences are significantly above zero for all stimuli.

after stimulus onset on a trial-by-trial basis. A receiver operant characteristic (ROC) analysis was performed on the obtained activity distributions, and the area under the ROC curve (AUC) was taken as a measure of stimulus detection sensitivity (Green and Swets 1966).

A local activity contrast (LAC) was calculated by dividing the absolute difference in spike count between subsequent trials by their mean spike count. Since this measure turned out to be strongly correlated with the average spike count on the included trials, we derived the theoretical relationship between these two variables under the assumption of Poisson spiking (Bair et al. 1994; Maimon and Assad 2009). This relationship was then used to divide each recorded LAC value by the expected value of LAC (<LAC>) at each level of activity. If this ratio is 1.0, the observed LAC corresponds to the expected LAC for Poisson spiking. LAC values > 1.0 indicate more trial-to-trial spiking variability than a Poisson process, whereas LAC values < 1.0 indicate that the spike counts in subsequent trials are more regular than a Poisson process.

To calculate the behavior of LAC under the null hypothesis of Poisson firing (*Eq. 1*) with spike rate λ, we focus on the absolute spike count difference δ between subsequent trials at a fixed total spike count n (*Eqs. 2* and *3*). Expressed in these terms, the LAC can be defined as denoted in *Eq. 4*.

$$p[k] = \lambda^k e^{-\lambda}/k! \quad (1)$$

$$\delta = k_1 - k_2 \quad (2)$$

$$n = k_1 + k_2 \quad (3)$$

$$LAC = 2|\delta|/n \quad (4)$$

A useful classical result is that the conditional spike count distribution for a trial (k_1) under a fixed total spike count n is the binomial distribution of k_1 hits in n attempts with probability 0.5 (*Eq. 5*). Fixed n also implies that the spike count difference δ is directly related to both the single trial spike count and the total spike count (*Eq. 6*). As a result, the distribution of δ is a scaled and shifted version of the trial spike count binomial, such that it has mean zero and variance n.

$$\mathbb{P}[k_1|n] = 2^{-n}\binom{n}{k_1} \quad (5)$$

$$\delta = 2k_1 - n \quad (6)$$

For reasonably large spike counts, this δ distribution becomes Gaussian, so we can easily compute the expected spike count difference (*Eq. 7*), and the expected LAC, conditional upon the total spike count (*Eq. 8*). Trivially, one can also express the result in terms of the spike count mean: $m = n/2$.

$$\langle |\delta| \rangle = 2\int_0^\infty \frac{\delta}{\sqrt{2\pi n}} \exp\left(-\frac{\delta^2}{2n}\right) d\delta = -\sqrt{\frac{2n}{\pi}} \exp\left(-\frac{\delta^2}{2n}\right)\Bigg|_0^\infty = \sqrt{\frac{2n}{\pi}} \quad (7)$$

$$\langle LAC \rangle = 2\sqrt{\frac{2}{\pi n}} = \sqrt{\frac{2}{\pi m}} \quad (8)$$

For the analysis of precise spike timing we used the timestamps of spikes relative to stimulus onset. A cost-based distance estimate between the spike trains of subsequent stimulus presentations was calculated with the metric developed by Victor and colleagues (Victor 2005; Victor and Purpura 1996). This method estimates the difference in temporal structure of two spike trains (D^{spike}) as the minimal overall cost of a set of elementary operations (inserting, removing, or shifting a spike in time) that are needed to transform one spike train into the other (for details, see Victor 2005). While the insertion and removal of a spike are both assigned a fixed value of 1, the cost of shifting a spike in time is defined relative to the distance it needs to be shifted. The results reported here were obtained with a cost for shifting a spike of 0.2 ms^{-1}, meaning that when a spike would require a shift of >10 ms to reach its new position, it would be more cost-efficient to remove and insert a spike rather than displace it. The D^{spike} obtained with this analysis was then divided by the number of spikes to obtain a measure of cost-based distance per spike (D^{spike}/spike).

LFP recordings were low-pass filtered at 250 Hz before further analysis. The traces were then downsampled to 2 kHz, and second-order Butterworth notch filters were applied at 50 Hz and 100 Hz. Around each spike, the samples from 2 ms before to 8 ms after the spike were removed and replaced with an interpolation of the surrounding LFP trace. Instances where the LFP trace amplitude exceeded the mean amplitude with >6 standard deviations were labeled as artifacts, and trials that contained artifacts were removed from the data analysis. Spectral analysis of spike-field coherence (SFC) was performed on this signal with a multitaper Fourier analysis method (Mitra and Bokil 2007; Mitra and Pesaran 1999) performed with the open-source Chronux 2.0 toolbox (Bokil et al. 2010) for MATLAB, which is available at **http://chronux.org**. SFC spectrograms for LFP frequencies up to 300 Hz were estimated in 200-ms moving windows zero-padded to 256 ms and moving with 5-ms increments from 250 ms before stimulus onset to 2 s after stimulus offset, using 2 tapers (time-bandwidth product TW = 1) for frequencies up to 80 Hz and 5 tapers (TW = 3) for frequencies between 80 and 300 Hz.

Control for block and fixation duration. The total amount of stimulus drive in our experimental design was kept equal for the different conditions by using approximately the same number of stimulus presentations for each block while varying the off-period duration. This choice of equal stimulus drive per block does, however, result in a difference in total duration of blocks with different off-periods. Furthermore, since the monkey was required to maintain fixation throughout a sequence of stimulus presentations, the number of stimuli that can subsequently be presented in an equally long period of fixation depends on the off-period as well. To check whether these factors could potentially influence our results we reanalyzed the data from the blocks with the shortest off-periods to compare the spike-based measures reported in this study for four specific subsets of the data. The first subset included all valid trials (as described above and reported in RESULTS). The second and third subsets only included the first and last 10 stimulus presentations of a block of trials, respectively. Any effect of block duration should show up as a difference between these subsets. In the fourth subset, we only included the first three trials after the monkey initiated a period of fixation. Contrasting the results with this subset against the results with all valid trials offers a control for a possible effect of fixation duration.

RESULTS

To investigate the effects of intermittent stimulus presentation on neuronal response properties in area MT of the rhesus macaque, we presented two monkeys with blocks of stimulus sequences in which the stimulus was repeatedly displayed for 500 ms ("on") and removed from view for a fixed blank duration ("off") that could be 250, 500, 1,000, or 2,000 ms (Fig. 1*A*). This off-duration was kept constant within a block of ~100 stimulus repetitions. In correspondence with previous behavioral studies on perceptual stabilization, we used an ambiguously rotating cylinder stimulus for which there are two perceptual interpretations with opposite rotation directions (Klink et al. 2008). To discern any general effect of repeated stimulus presentation from more specific effects related to the presence of a visual ambiguity, we included two additional control stimuli in our experimental protocol. These were *1*) dynamic random noise patches that contained all motion directions in balanced proportions and *2*) unambiguous, "opaque" cylinders (Freeman and Driver 2006) that contained only one motion direction in the preferred direction of the recorded neuron and no perceptual ambiguity. Responses to the sequences of these stimuli were obtained from 94 single units in area MT of two macaque monkeys (46 from *monkey S* and 48 from *monkey A*).

Spike rate and adaptation. When an MT neuron is continuously, or repeatedly, driven by the same type of input its responsiveness will decrease, a phenomenon known as neuronal adaptation (Kohn 2007; van Wezel and Britten 2002). The adapted responsiveness will recover back to baseline values when stimulation stops, but this may take some time. During intermittent stimulus presentation, the length of the off-period determines the extent to which a neuron will recover from adaptation evoked by the previous stimulus presentation. Figure 1*B* displays the average PSTHs for the recorded neurons, split up for the three different stimuli (panels) and four off-durations (colors within a panel). It is immediately clear that the average response amplitude increases with increasing off-duration for all three stimuli (Spearman rank correlations of off-duration vs. average spike rate during stimulus presentation over all trials within a stimulus type: all $r > 0$, all $P < 0.001$). This effect is clearly visible in both the transient phase of the response (defined as the first 200 ms after a 50-ms fixed latency, labeled "T" in Fig. 1*B*) and in the sustained phase (defined as the last 300 ms, labeled "S" in Fig. 1*B*) for the ambiguous cylinder and dynamic random noise stimuli. In the transient phase of the response to opaque cylinders, it is less pronounced but still significant.

The difference in average response magnitude over full on-periods is largest for a comparison between the blocks with shortest and longest off-durations. If we directly compare these average responses for the shortest (250 ms) and longest (2,000 ms) off-durations for individual cells, we notice that for practically all recorded cells and for all stimuli, long off-durations yield higher spike rates than short off-durations (Fig. 1, *C* and *D*) (paired *t*-test, $P < 0.001$). While this effect is exactly what one would expect from general adaptation, it also presents a potential confound and requires additional analyses of the effects of off-durations on response variability. We take these possible adaptation effects into account by consistently checking to what degree any influence of off-duration on response variability could be explained by response magnitude.

Fano factors. It has recently been shown that in a wide range of cortical areas, including area MT, stimulus onset reduces the response variability expressed in the Fano factor (FF) (Churchland et al. 2010). FF is calculated by dividing the spike count variance of a response by its mean (σ^2/μ). We calculated FFs for our stimuli and off-durations both by directly dividing the variance to the mean in a 70-ms sliding windows moving in 10-ms increments and by applying the "mean-matched" method introduced by Churchland et al. (2010). Since these two methods resulted in qualitatively similar results (Fig. 2*A*, *inset*, *bottom*), we performed the additional analyses on the directly calculated FFs that are based on more data points.

For all three stimulus types, stimulus onset clearly reduced the FF, but the extent to which the FFs decreased depended on the duration of the off-period (Fig. 2*A*). For the ambiguous and opaque cylinders this notion held for both the transient and sustained phases (Spearman rank correlation, ambiguous: $r_{trans} < 0$, $P_{trans} < 0.01$; $r_{sust} < 0$, $P_{sust} < 0.02$; opaque: $r_{trans} < 0$, $P_{trans} < 0.05$; $r_{sust} < 0$, $P_{sust} < 0.02$), while for the dynamic noise patches only the transient phase showed a significant off-duration dependence ($r_{trans} < 0$, $P_{trans} < 0.03$; $r_{sust} < 0$, $P_{sust} = 0.10$). A comparison of the average FF during the full stimulus presentation for the longest and shortest off-durations (Fig. 2, *B* and *C*) reveals that for virtually all cells the FF is lower for the long off-duration in all three stimuli (paired *t*-test, $P < 0.001$). The FF, by defini-

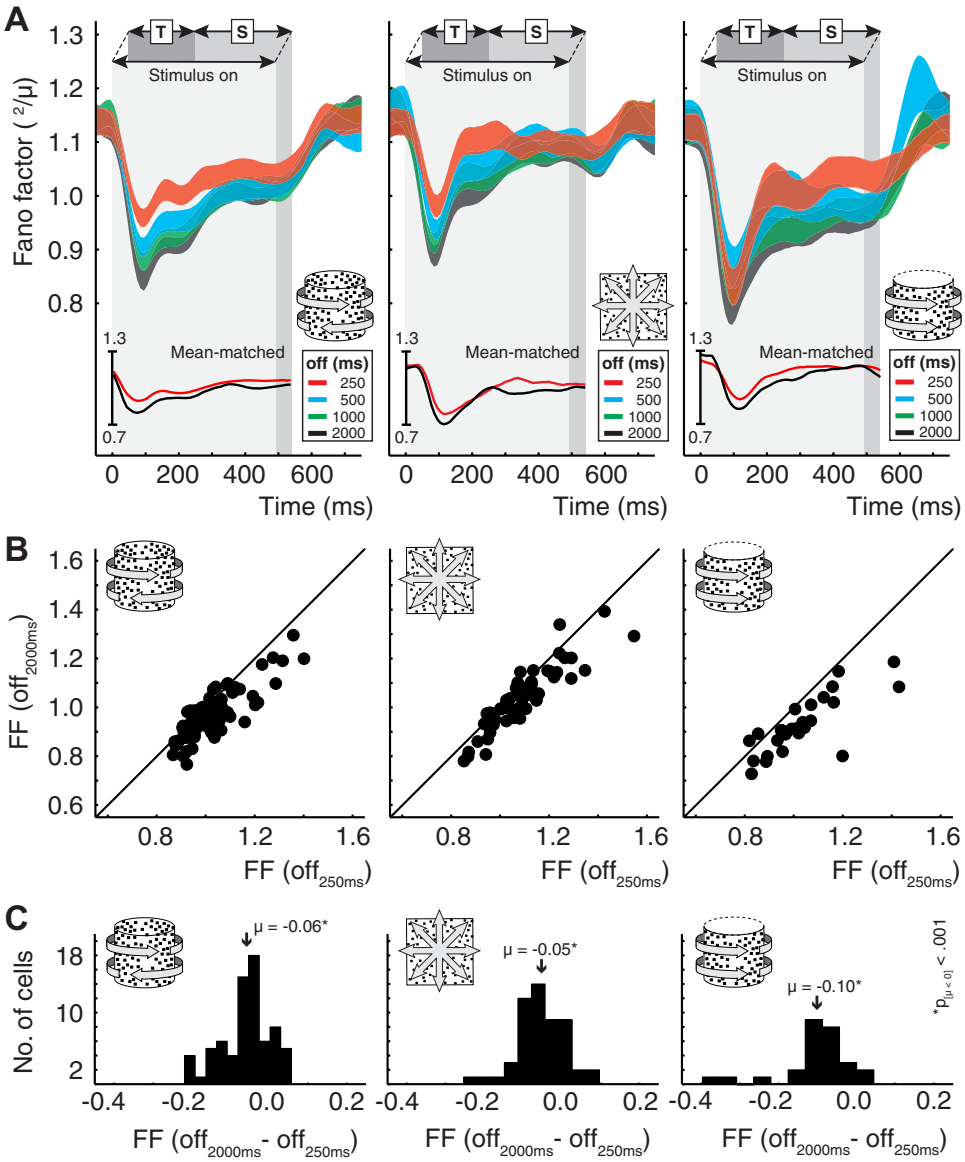

Fig. 2. Fano factors (FFs) decrease differentially at stimulus onset. *A*: averaged FFs for different stimuli (panels) and off-durations (colors). FFs were calculated in 10-ms bins aligned to stimulus onset and averaged over cells (n_{amb_cyl} = 82, 80, 79, 67; n_{dyn_noi} = 56, 61, 58, 55; n_{op_cyl} = 29, 30, 29, 29 for the 4 off-durations in increasing order, respectively). For plotting purposes, the data were smoothed with a 50-ms moving average window. Line thickness indicates the average value ± SE. Gray rectangular area marks the moment of stimulus presentation. The transient and sustained phases of the response are marked with "T" and "S," respectively. Mean-matched FFs (see MATERIALS AND METHODS for details) are plotted in *inset* at *bottom* for the shortest and longest off-durations (n_{amb_cyl} = 63, 41; n_{dyn_noi} = 52, 46; n_{op_cyl} = 24, 14). *B*: average FFs during full stimulus presentations for the shortest vs. the longest off-duration split up by stimulus type (panels). Dots are individual cells (n_{amb_cyl} = 67; n_{dyn_noi} = 55; n_{op_cyl} = 29). *C*: distributions of differences in the average FF during stimulus presentation with longest and shortest off-duration over all cells. Mean differences are significantly below zero for all stimuli.

tion, depends both on the mean and the variance of the neural response. The observed differences in FF for the different off-period durations could thus be compromised by the difference in response magnitude that also varied with the off-period duration. To control for this potential confound, we performed an additional analysis of variance with the average spike count as a continuous predictor variable and the off-period as a categorical predictor variable. This specific analysis tells us whether response magnitude significantly influenced the FF and, if so, the proportions of the total variance in FF explained by response magnitude and off-period duration, respectively. The result revealed that response magnitude was not a significant factor for the observed differences in FF (ANCOVA, $P_{amb\_cyl} = 0.53$, $P_{dyn\_noi} = 0.44$, $P_{opa\_cyl} = 0.74$).

It has been argued that the drop in FF at stimulus onset reflects some kind of stabilization of cortical networks when they are driven (Churchland et al. 2010). Furthermore, it has been demonstrated that the decline in FF when a stimulus enters the receptive field of a V4 neuron is stronger when this stimulus is attended than when it is not attended (Mitchell et al. 2007). This suggests that attention may cause an additional reduction of response variability that facilitates a maximized neuronal signal-to-noise ratio (Mitchell et al. 2007). Our results demonstrate that such a stronger decrease in neuronal response variability similarly exists for intermittent stimulus presentations without explicit attentional demands but with increasingly longer off-durations.

Both the increases in response magnitude and the reduction in FF with longer blank intervals could theoretically improve the signal-to-noise ratio and help areas downstream from MT to decode stimulus presentations. To check whether this was indeed the case we performed a ROC analysis (Green and Swets 1966) in which we contrasted the spiking activity in the 100 ms before stimulus presentation with the 50–150 ms after stimulus onset. The AUC was then taken as an indication of stimulus detection sensitivity and compared across conditions (Fig. 3). For ambiguous stimuli, AUC values significantly increased with off-duration (Spearman rank correlation: $r > 0$, $P < 0.05$) (Fig. 3*A*). For dynamic noise stimuli, there was a similar trend ($r > 0$, $P = 0.06$), but AUC values for opaque cylinders were generally high, even at short off-duration, leaving no significant effect of off-duration here ($P = 0.55$). A paired comparison of AUC values with the shortest and longest off-durations confirmed these findings (Fig. 3, *B* and *C*; $P_{amb\_cyl} < 0.001$, $P_{dyn\_noi} < 0.01$, $P_{opa\_cyl} = 0.21$). To control for any effects of differences in mean firing rate between cells, the same analysis was performed on z score units of spiking, yielding very similar results (Spearman rank correlations: $r_{amb\_cyl} > 0$, $P_{amb\_cyl} < 0.05$; $r_{dyn\_noi} > 0$, $P_{dyn\_noi} = 0.06$; $P_{opa\_cyl} = 0.55$; paired t-test: $P_{amb\_cyl} < 0.05$, $P_{dyn\_noi} = 0.06$, $P_{opa\_cyl} = 0.55$).

Local activity contrast. Whereas FFs provide a nice estimate of response variability over the full sequence of stimulus presentations and the associated responses, we would also like

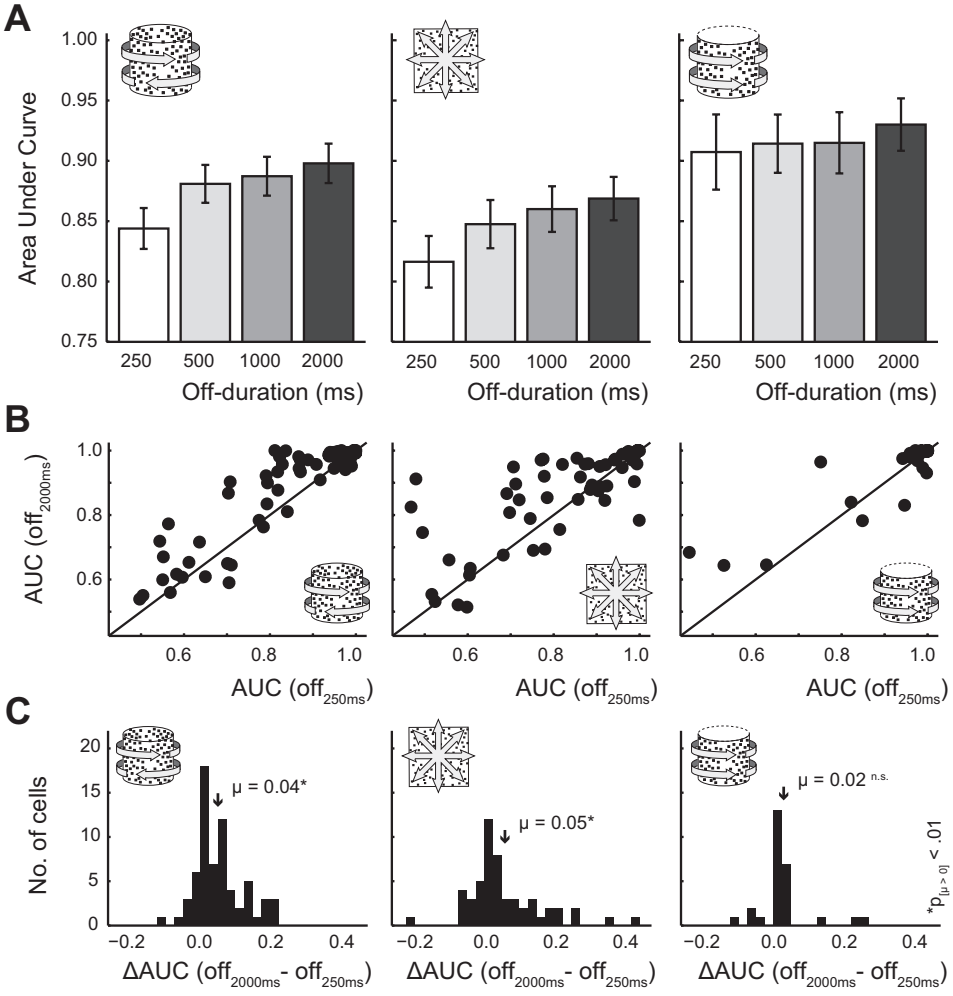

Fig. 3. Receiver operant characteristic (ROC) analysis. *A*: area under curve (AUC) values for different stimuli (panels) and off-durations (gray shades) calculated with an ROC analysis that contrasts the activity in the 100-ms period prior to stimulus presentation and the 50–150 ms period after stimulus onset and averaged over cells ($n_{amb\_cyl} = 82, 80, 79, 67$; $n_{dyn\_noi} = 56, 61, 58, 55$; $n_{op\_cyl} = 29, 30, 29, 29$). *B*: average AUC for the shortest vs. the longest off-duration split up by stimulus type (panels). Dots are individual cells ($n_{amb\_cyl} = 67$; $n_{dyn\_noi} = 55$; $n_{op\_cyl} = 29$). *C*: distributions of differences in the average AUC with longest and shortest off-duration over all cells. Mean differences are significantly above zero for ambiguous cylinders and dynamics noise, whereas the generally high AUCs for opaque cylinders negate any potential differences for opaque cylinders. n.s., Not significant.

to obtain a more temporally local measure of trial-to-trial response variability. To this end we calculated the LAC, which we defined as the absolute spike count difference between subsequent trials divided by the mean activity of these two trials (*Eq. 9*). In this equation, k_n denotes the spike count in the first trial of the pair and k_{n+1} the spike count during the second trial. The LAC can theoretically take values between 0 (when there is an equal number of spikes on both trials) and 2 (when there are no spikes on one of the two trials).

$$LAC = \frac{|k_{n+1} - k_n|}{(k_{n+1} + k_n)/2} \quad (9)$$

Figure 4*A* demonstrates that the LAC value significantly depends on the duration of the off-interval for all stimuli, with a lower LAC when off-periods are longer (Spearman rank correlations; all $r < 0$, all $P < 0.05$). The LAC values are relatively low in general, indicating that subsequent trials do not differ in their spike count all that much. If the shortest and longest off-durations are contrasted (Fig. 4, *B* and *C*), we can clearly see that for practically all cells the longer off-duration is correlated with the lower LAC (paired *t*-test, all $P < 0.01$).

One concern with this definition of local activity contrast is that the LACs are strongly correlated with the average spike count on the two trials (Spearman rank correlations; all $r < 0$, all $P < 0.0001$). Since we already demonstrated that the duration of the off-interval significantly influences the average spike count, it remains questionable whether there is any direct effect of off-period duration on LAC, or whether the effect of

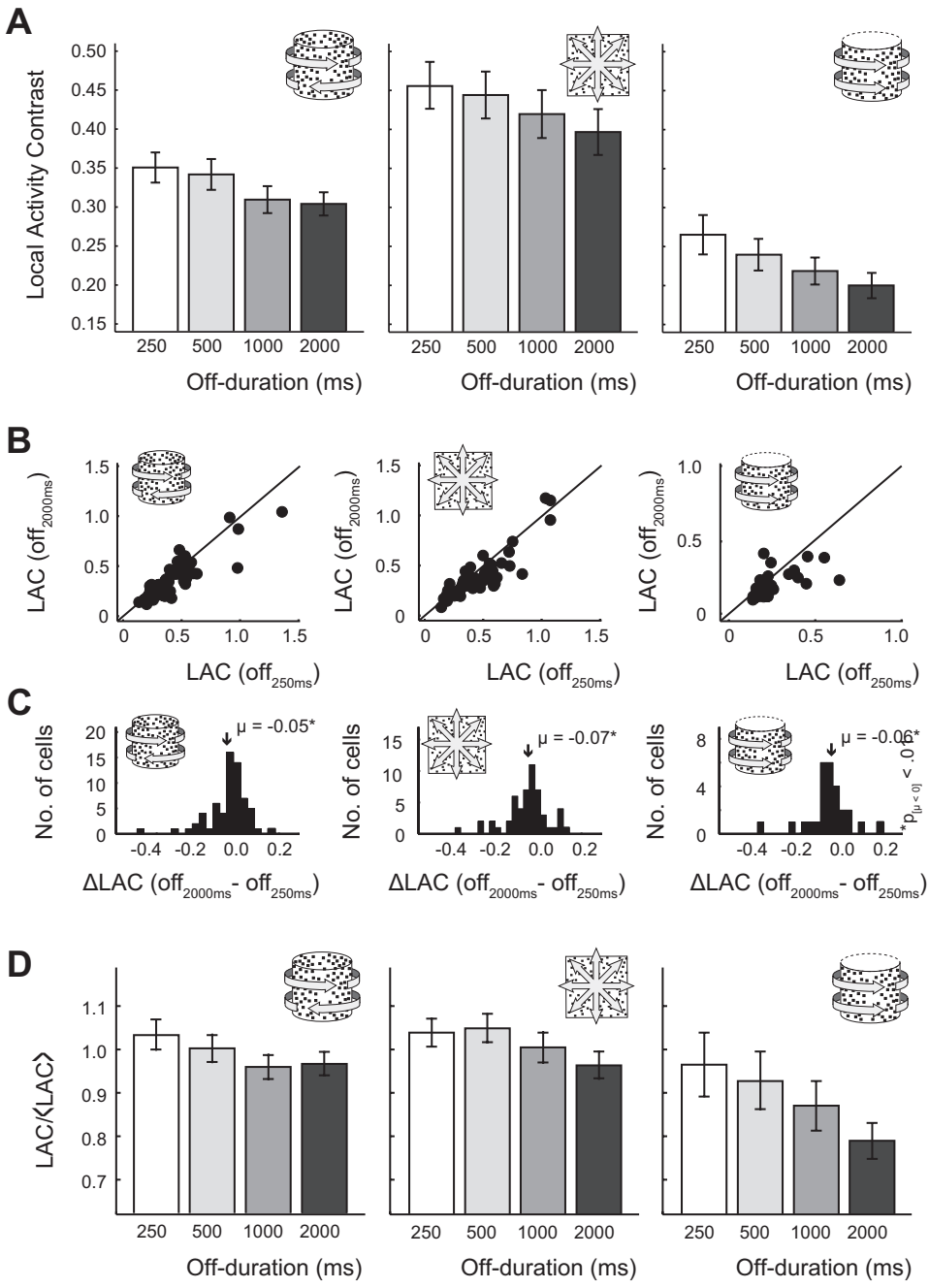

Fig. 4. Local activity contrast (LAC) decreases with off-duration. *A*: LAC, calculated as the absolute spike count difference between subsequent stimulus presentations divided by the average spike count on these subsequent trials, averaged over the same cells as presented in Fig. 2 and plotted against the off-duration for the 3 different stimuli. Error bars are SE. *B*: LAC values on the shortest off-duration of 250 ms contrasted with the longest off-duration of 2,000 ms for individual cells (dots) and different stimuli (panels) ($n_{amb\_cyl} = 67$, $n_{dyn\_noi} = 55$, $n_{op\_cyl} = 29$). *C*: distributions of LAC differences between trials with the longest and shortest off-durations within a single cell. *D*: ratio of the measured LAC and the Poisson-predicted LAC values (<LAC>) plotted for the different stimuli and off-durations.

off-period is a completely indirect effect that acts through a change in response magnitudes. To answer this question, we again performed an analysis of variance with response magnitude incorporated as a continuous grouping variable. This analysis revealed that a significant proportion of the variance in LAC could indeed be explained by differences in response magnitude (ANCOVA, all $P < 0.01$; $\omega^2_{amb\_cyl} = 0.12$, $\omega^2_{dyn\_noi} = 0.15$, $\omega^2_{opa\_cyl} = 0.07$). The off-period duration by itself, however, did also have a small but highly significant influence on the LAC (all $P < 0.01$; $\omega^2_{amb\_cyl} = 0.02$, $\omega^2_{dyn\_noi} = 0.01$, $\omega^2_{opa\_cyl} = 0.03$), meaning that the difference in observed LAC for the different off-periods does not solely depend on the difference in response magnitude.

We may visualize the remaining effect of off-period duration independent of response magnitude by estimating the expected relation between response magnitude and LAC. This relation can be approximated if we assume that our neuron's spike counts (k) resemble independent samples from the same Poisson distribution (Bair et al. 1994; Maimon and Assad 2009). The assumption of Poisson spiking is, of course, an oversimplification and inconsistent with neuronal response features such as bursting or refractoriness. It is further challenged by our findings of off-duration-dependent FFs, but it is nevertheless a very common interpretation of the spike generation mechanism that may provide an indication of the dependence of the LAC on off-duration. The Poisson-predicted LAC values can be derived to follow *Eq. 10* (for details on the derivation see METHODS AND MATERIALS).

$$\langle LAC \rangle = \frac{2}{\sqrt{\pi\left(k_1 + k_2/2\right)}} \qquad (10)$$

With this predicted LAC, we can calculate the ratio of the measured and predicted LAC for every pair of trials individually (LAC/<LAC>). A value smaller than 1.0 would indicate less variability in trial-to-trial spike counts than predicted for a Poisson process, whereas a value larger than 1.0 would imply more variability. Consistent with our FF findings, Fig. 4*D* demonstrates that LAC/<LAC> decrease with increasing off-duration, indicating that indeed trial-to-trial variability is lower when stimulus sequences are presented with longer intermittent blank intervals. For ambiguous cylinders and dynamic noise, LAC/<LAC> is above 1.0 for the shortest off-interval and below 1.0 for the longest off-periods. The resolution of perceptual ambiguity in the former and broad motion direction content of the latter could be responsible for this higher initial trial-to-trial variability that appears to stabilize when blank durations increase. The opaque cylinders that contain only one motion direction and no inherent ambiguities show an overall lower LAC/<LAC>, but the stabilizing effect of increasing off-duration is also clearly present there.

Spike timing precision. Both the FF analysis and the LAC analysis consider merely the number of spikes in a given time interval, not their exact moments of incidence. Decreases in neuronal response variability may, however, also be reflected in an increased regularity in the timing of spike trains evoked by subsequent stimulations (Maimon and Assad 2009). To investigate this possibility, we calculated a cost-based distance estimate to quantify the similarity in temporal spike train structure between responses to subsequent stimulus presentations (Victor 2005; Victor et al. 2007). In this analysis, one spike train was stepwise transformed into another one with a specific cost assigned to each elementary step needed to get there. Removing and inserting a spike had a fixed cost of 1, while shifting a spike in time had a cost of 0.2 per millisecond that it needed to be shifted. The minimal overall cost D^{spike} needed to transform one spike train into the next was then used to calculate the cost per spike (D^{spike}/spike) for all stimuli and blank durations. Figure 5*A* plots D^{spike}/spike for the different stimuli and off-durations, averaged over all stimulus presentations. Spike train distance significantly decreased with increasing off-duration for ambiguous cylinder stimuli (Spearman rank correlation, $r < 0$, $P < 0.001$) and dynamic noise patches ($r < 0$, $P < 0.01$), while it showed a clear trend for unambig-

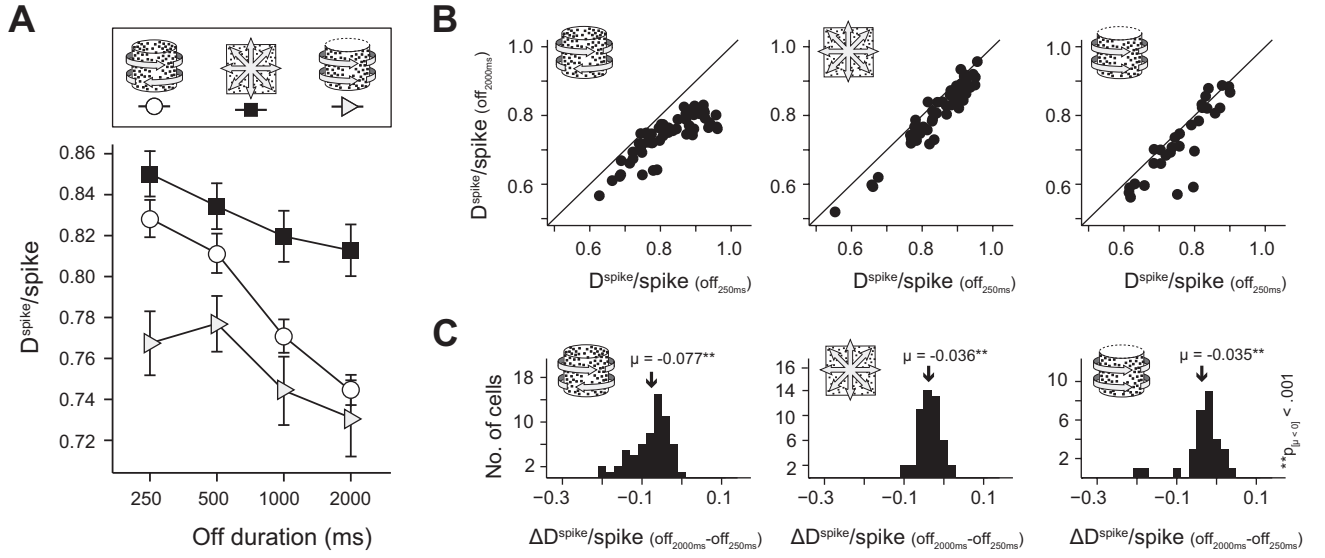

Fig. 5. Spike train distance. *A*: cost-based spike train distances (D^{spike}) calculated as the average cost for the stepwise transformation of one spike train into the next and normalized to the total number of spikes. D^{spike}/spike values are averaged over the same cells as presented in Figs. 2–4 and plotted against off-duration for the 3 different stimuli. Error bars are SE. *B*: D^{spike}/spike values with the shortest off-duration contrasted against those with the longest off-duration for individual cells ($n_{amb\_cyl} = 67$, $n_{dyn\_noi} = 55$, $n_{op\_cyl} = 29$). *C*: distributions over cells of the D^{spike}/spike value differences plotted in *B*.

uous opaque cylinder stimuli ($r < 0$, $P = 0.07$). Interestingly, the average D^{spike}/spike values for the unambiguous opaque cylinder are a lot lower than for the dynamic random noise patches, while D^{spike}/spike values for ambiguous cylinders are similar to those of dynamic noise at short blank intervals but more similar to those of opaque cylinders at long blank periods. This transition may be related to the fact that intermittently presented ambiguous stimuli are perceptually unstable at short off-periods (high perceptual alternation probability) but become increasingly stable with longer stimulus interruptions (high perceptual repetition probability).

When the average D^{spike}/spike values of the shortest and longest off-periods are contrasted for individual cells (Fig. 5, *B* and *C*), the D^{spike}/spike value for the longest off-period is lower in most cells for all three stimuli, an effect that is significant for the population of recorded neurons (paired *t*-tests, all $P < 0.001$). We again checked whether the D^{spike}/spike differences for the different off-periods were merely an indirect effect of the differences in spike count or whether the off-period duration had an additional effect by performing an analysis of variance with average spike count as a continuous grouping variable. While this analysis revealed that the cost-based spike train distance was for a significant proportion influenced by response magnitude (ANCOVA, all $P < 0.001$; $\omega^2_{amb\_cyl} = 0.05$, $\omega^2_{dyn\_noi} = 0.38$, $\omega^2_{opa\_cyl} = 0.50$), an additional effect of off-duration independent of response magnitude was highly significant as well (all $P < 0.01$; $\omega^2_{amb\_cyl} = 0.21$, $\omega^2_{dyn\_noi} = 0.05$, $\omega^2_{opa\_cyl} = 0.04$).

Control for block and fixation duration. Sequences of stimulus presentations with different intermittent off-durations were kept equally long in terms of number of stimulus repetitions. Consequently, they differed in their total duration and in the average number of stimuli presented during a continuous period of uninterrupted fixation. To control whether these differences could have affected our results, the data from blocks with the shortest off-periods were reanalyzed to allow a comparison of the spike-based measures reported in this study among four subsets of the data. The first subset included all valid trials (as described above in RESULTS). The second and third subsets controlled for the effect of block duration and only included the first and last 10 stimulus presentations of a block of trials, respectively. The fourth subset included only the first three trials after the monkey initiated a period of fixation and offers a control for a possible fixation duration effect.

While we did find some adaptation effects on response magnitude (first 10 trials vs. last 10 trials: $P_{amb\_cyl} < 0.01$, $P_{dyn\_noi} = 028$, $P_{opa\_cyl} < 0.05$; first 3 trials after fixation onset vs. all trials: $P_{amb\_cyl} < 0.01$, $P_{dyn\_noi} = 0.23$, $P_{opa\_cyl} = 0.22$), there were no effects on any of the variability measures. FFs were not significantly different between the first and last 10 trials of a block ($P_{amb\_cyl} = 0.50$, $P_{dyn\_noi} = 0.27$, $P_{opa\_cyl} = 0.71$), or between the subset of trials right after fixation compared with the full set of trials ($P_{amb\_cyl} = 0.09$, $P_{dyn\_noi} = 0.20$, $P_{opa\_cyl} = 0.41$). The same was true for the D^{spike}/spike (first 10 trials vs. last 10 trials: $P_{amb\_cyl} = 0.69$, $P_{dyn\_noi} = 0.95$, $P_{opa\_cyl} = 0.66$; first 3 trials after fixation onset vs. all trials: $P_{amb\_cyl} = 0.27$, $P_{dyn\_noi} = 0.82$, $P_{opa\_cyl} = 0.56$) and the LAC (first 10 trials vs. last 10 trials: $P_{amb\_cyl} = 0.89$, $P_{dyn\_noi} = 0.70$, $P_{opa\_cyl} = 0.41$; first 3 trials after fixation onset vs. all trials: $P_{amb\_cyl} = 0.68$, $P_{dyn\_noi} = 0.57$, $P_{opa\_cyl} = 0.38$). These controls provide a relatively good indication that the difference in block duration between different off-period conditions and/or the number of stimulus presentations during a continuous period of fixation did not have a significant impact on our results.

Spike-field coherence. All the spike-based analyses indicated that neuronal responses are less variable when intermittently presented stimuli are separated by longer off-intervals. However, the neuronal mechanisms by which this reduction in variability is established remain unclear. It has been shown that spiking variability in sensorimotor cortex is lower in the presence of oscillations in LFP (Murthy and Fetz 1996). A straightforward hypothesis would thus be that interactions between neurons in a local cortical network in area MT somehow lead to lower spiking variability, perhaps by time-locking the spikes of the single units in the network to each other's activity or to an additional shared neural signal (Churchland et al. 2010; Kelly et al. 2010; Sussillo and Abbott 2009). Analysis of the LFPs that we recorded simultaneously with our spiking data may provide some clues about the role of this local cortical network (Gawne 2010; Katzner et al. 2009). Since our data were recorded with single electrodes, we cannot directly correlate the activity patterns of multiple simultaneously active neurons. We can, however, use the spiking activity and LFPs that were recorded from the same electrode to search for clues of network effects (Belitski et al. 2008; Fontanini and Katz 2008; Fries et al. 2007; Logothetis 2003; Singer and Gray 1995). To this end, we calculated SFC spectrograms for all stimuli and contrasted the spectrograms obtained with the shortest off-duration of 250 ms with those from blocks where the off-duration was 2,000 ms. If the local cortical network uses the LFP signal to increase the reliability of information transfer in spike trains, we would expect to see shifts in the SFC spectrograms occurring parallel to the changes in spiking variability.

Time-resolved SFC spectrograms are presented in Fig. 6 and reveal how the coherence between spikes and the LFP is modulated by stimulus presentation. Compared with coherence values during the intermittent blank period, stimulus presentations increase the coherence in the high gamma frequency range (>80 Hz) while coherence decreases for lower frequencies (10–50 Hz). This modulation is even more clearly visible in Fig. 7*A*, where the average SFC is plotted over time for the low beta/gamma (10–50 Hz) and high gamma (80–120 Hz) frequency bands, normalized to the average SFC at stimulus onset (only shown for ambiguous cylinder stimuli, but the same pattern exists for other stimuli). The counterphase modulations of SFC in the two frequency bands suggest that during stimulus presentation, the coherence between spikes and LFP shifts toward higher frequency components of the LFP. If the average SFC during stimulus presentation is contrasted with that during the blank period (Fig. 7*B*, only shown for ambiguous cylinders), there is a clear shift in coherence from lower toward higher frequencies. Both the suppression of coherence in the lower frequency band during stimulus presentation and the increase in coherence for the higher frequencies were statistically significant for all stimuli and off-durations (paired *t*-tests over cells, comparing the average coherence during stimulus presentation between 200 and 400 ms after stimulus onset with the average coherence during the off-period be-

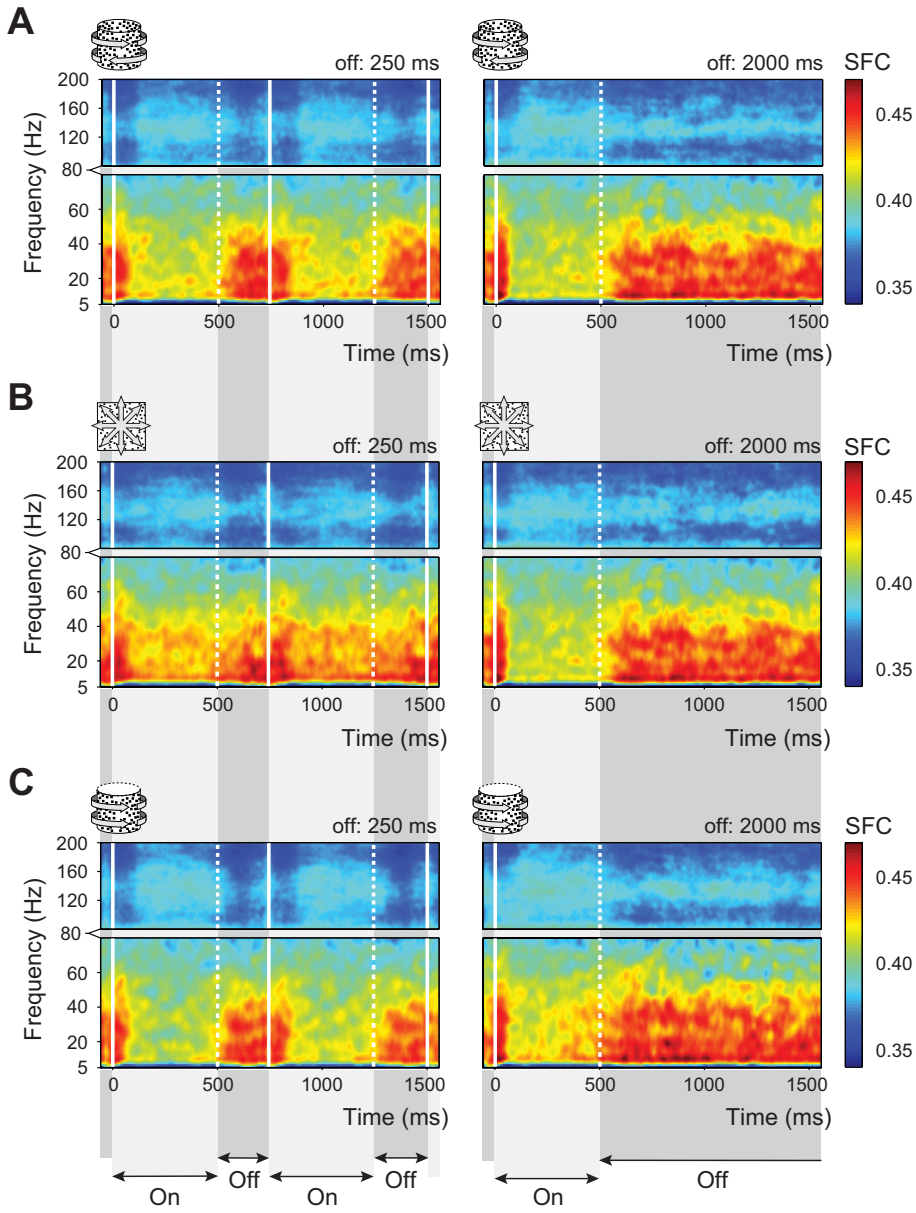

Fig. 6. Spike-field coherence (SFC) spectra. *A–C*: cell-averaged time-resolved SFC spectra during presentation of the 3 different stimuli with intermittent off-durations of 250 ms (*left*; $n_{amb\_cyl} = 64$, $n_{dyn\_noi} = 54$, $n_{op\_cyl} = 29$) and 2,000 ms (*right*; $n_{amb\_cyl} = 62$, $n_{dyn\_noi} = 54$, $n_{op\_cyl} = 29$). Stimulus onset is indicated with solid vertical white lines and stimulus offset with dotted white vertical lines, and periods where stimuli were either "on" or "off" are represented by the light and dark gray areas behind the plots, respectively.

tween 50 and 250 ms after stimulus offset: 10–50 Hz, all $P < 0.01$; 80–120 Hz, all $P < 0.05$).

Comparison of coherence values during stimulus presentations between off-durations also yielded interesting results. Longer off-periods were generally associated with both higher coherence in the 80–120 Hz band and lower coherence in the 10–50 Hz band compared with short off-durations (Fig. 7, *C* and *D*). While this difference was relatively small, it was highly significant for both ambiguous and opaque cylinder stimuli (paired *t*-test within cells, $P < 0.01$). For dynamic noise stimuli, the difference was only significant for the high-frequency coherence values ($P < 0.01$), not for the lower-frequency band ($P = 0.20$).

If temporal correlations between the LFP and spikes are based on data from a single electrode, spurious correlations in frequencies > 50 Hz can arise from contamination of the LFP signal by the spectral contents of the spike waveforms (Zanos et al. 2011). As a result, increases in spike rate can artificially increase the apparent coherence between spikes and LFPs recorded from the same electrode. Since the difference in SFC that we report for the frequencies between 80 and 120 Hz coincide with an increased spike rate, this could potentially confound this aspect of our results. While our method of LFP interpolation around spike moments is a commonly used approach for removing spikes from the LFP trace (Galindo-Leon and Liu 2010; Jacobs et al. 2007; Okun et al. 2010), it was recently shown to be far from perfect (Zanos et al. 2011). A more efficient Bayesian spike waveform subtraction algorithm (Zanos et al. 2011) requires a wide-band LFP signal with a higher sampling rate than we have available in our data. We performed two additional analyses to investigate the potential presence of spurious correlations in the 80–120 Hz frequency band of our SFC data. ANCOVAs on SFC data with spike rate as continuous grouping variable revealed that there was indeed a strong effect of spike rate for all stimuli (all $P < 0.01$), indicating that spurious correlations play a significant role in

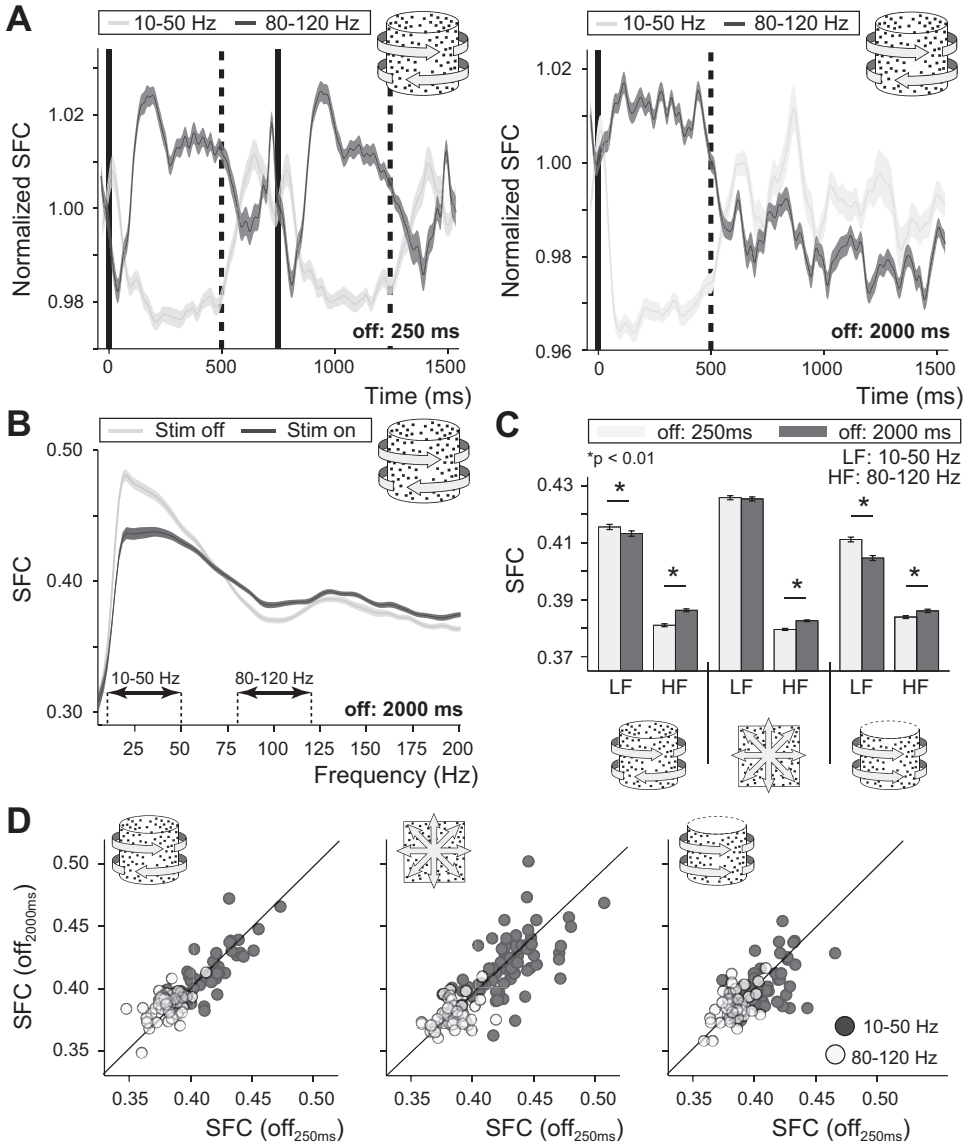

Fig. 7. Modulation of SFC. *A*: cell-averaged fluctuations of SFC in the low beta/gamma (10–50 Hz, light gray line) and high gamma (80–120 Hz, dark gray line) ranges during presentation and removal [for 250 ms (*left*) or 2,000 ms (*right*)] of an ambiguous rotating cylinder. The SFC within each frequency band is normalized to the average SFC at stimulus onset. Shaded areas represent SE. *B*: population-averaged SFC spectrograms for the stimulus presentation period between 200 and 400 ms after stimulus onset ("Stim on," dark gray) and the 50–250 ms of the intermittent blank duration after stimulus offset ("Stim off," light gray) for sequences of ambiguous cylinders with off-durations of 2,000 ms. Shaded areas represent SE. *C*: population average of the stimulus-evoked coherence values in the lower (LF, 10–50 Hz) and higher (HF, 80–120 Hz) frequency bands for the shortest (250 ms) and longest (2,000 ms) off-periods for all 3 stimulus types ($n_{amb\_cyl} = 32$, $n_{dyn\_noi} = 42$, $n_{op\_cyl} = 38$). *D*: distributions over cells of the average coherence values plotted in *C*.

this part of the SFC results. However, the interaction between spike rate and off-duration was also significant for all stimuli (all $P < 0.05$), suggesting that our results do not completely depend on spike rate alone. To reveal effects of off-duration on SFC without the confounding factor of spike rate, we calculated SFC for mean-matched subsets of the data (Kaliukhovich and Vogels 2012). These mean-matched subsets of cells were equalized in spike rate by randomly removing single cells from the analysis until the groups of different off-duration had a similar mean spike rate. This mean-matched SFC analysis confirmed the effects reported for the entire cell population, with significant off-duration-dependent differences in SFC for all stimuli and in both frequency bands (ANOVA, 10–50 Hz: $P_{amb\_cyl} < 0.01$, $P_{dyn\_noi} < 0.05$, $P_{opa\_cyl} < 0.05$; 80–120 Hz: $P_{amb\_cyl} < 0.01$, $P_{dyn\_noi} < 0.01$, $P_{opa\_cyl} < 0.05$; $n_{amb\_cyl} =$ 48, 61, 50, 54; $n_{dyn\_noi} =$ 52, 59, 53, 53; $n_{opa\_cyl} =$ 21, 27, 24, 27).

Altogether, the presence of a stimulus, and thus of stimulus-evoked activity, appears to lock the spiking activity of MT neurons to higher frequencies of the LFP signal than is the case in the absence of stimulation. This effect is stronger with longer off-periods, which is consistent with the idea that spikes that occur on the basis of a higher frequency could potentially be placed with higher temporal precision and lower variability than spikes that are locked to lower frequencies of the LFP.

LFP activity in area MT in the higher gamma range reflects the motion direction and speed tuning properties that can also be observed in spiking data of single-unit recordings (Khayat et al. 2010; Liu and Newsome 2006). Furthermore, oscillations in the gamma range are considered related to the synchronization of activated neuronal ensembles (Fries et al. 2007). The stronger shift in SFC to higher-frequency components of the gamma cycle with longer off-durations could be related to network-based mechanisms that reduce response variability. The increased coherence between spikes and LFP of the neurons in the local network could perhaps also explain the increased regularity in spike timing as indicated by the decreased D^{spike}/spike values in our spike timing analysis.

DISCUSSION

It is common practice in systems neuroscience to investigate brain functioning with repeated stimulus presentations. Re-

sponses are generally averaged over trials to obtain an estimate of the mean response magnitude. However, the timing of repeated stimulus presentation can profoundly influence the evoked responses on individual trials. Whereas the straightforward reduction of responsiveness known as adaptation or fatigue has been known for a long time, our novel results demonstrate a more complex effect of intermittent motion stimulus presentation on neuronal response patterns. When interruptions between stimulus presentations of a standard duration were systematically increased, neuronal response variability became increasingly smaller. We carefully checked whether the adaptation-driven response magnitude effects sufficed to explain the response variability effects. Even though response magnitudes were sometimes correlated with the variability measures, there was always an additional effect of off-duration that was independent of response magnitude. These response stabilization effects independent of magnitude effects could be observed in spike rate variability measures, both over sequences of tens of stimulus presentations and between pairs of directly subsequent trials, as well as in the variability of precise spike timing patterns.

Network-driven variability reduction. A decline in neural variability in response to stimulus presentation has recently been demonstrated to occur with a broad range of stimuli and in many cortical areas of both anesthetized and awake behaving monkeys (Churchland et al. 2010). In this particular study, data from multielectrode recordings suggest that the reduction in variability is a network property, implying some stimulus-driven stabilization effect within cortical circuits. Gamma oscillations have long been suggested to play a role in the synchronization of neuronal activity within a cortical circuit (Fries et al. 2007), and the presence of gamma oscillations has been shown to reduce spiking variability in sensorimotor cortex (Murthy and Fetz 1996). In area MT, similar synchronization effects may very well underlie the observed reduction in response variability, even in measures as subtle as precise spike timing. Our SFC analysis suggests that the occurrence of spikes during stimulus presentation is more strongly synchronized to LFP oscillation in the high gamma frequency range (80–120 Hz) than during intermittent blank durations. This increase in SFC at high frequencies is accompanied by a decrease in coherence at lower beta/gamma frequencies (10–50 Hz), indicating a stimulus-evoked shift in the SFC. Furthermore, this shift toward SFC in higher LFP frequencies is more pronounced for longer off-durations where spiking variability was also shown to be lower, suggesting that the altered SFC may somehow be responsible for the more regular spiking patterns.

Functionally, a reduction of response variability improves the signal-to-noise ratio of the neural code and allows a more reliable information transfer between neurons or processing stages. This potential role for reduced variability is supported by the finding that attention enhances the reliability of neuronal responses in area V4 of the macaque more strongly by reducing variability than by increasing response magnitude (Mitchell et al. 2007). In our study, we did not ask the monkey to report perception because we wanted to record neuronal activity that primarily related to the visual stimulation. While we believe that there is no reason to assume a systematic influence of attention with this paradigm, it is theoretically possible that the monkeys' attentional load covaried with the off-duration and that at least some of the effects of off-duration are related to these differences in attentional load. It has been shown that in area MT stimulus-driven power increases in the gamma range of the LFP are stronger for attended than for unattended stimuli (Khayat et al. 2010). A multitaper analysis with the same settings as in the SFC analysis was performed on the LFP data alone and revealed no differences in stimulus-driven gamma-power (20–100 Hz) increases between the shortest and longest off-durations for any of our stimuli (paired *t*-test across cells, $P_{amb\_cyl} = 0.24$, $P_{dyn\_noi} = 0.98$, $P_{opa\_cyl} = 0.08$). We also analyzed whether any hints of attentional load differences between off-durations could be extracted from the animal's eye movement data and found no differences in either eye position or horizontal eye movement distance relative to the stimulus position (all $P > 0.11$). Vertical eye movements were not informative because they were heavily contaminated by pupil dilation differences in response to the changes in luminance evoked by stimulus presentation. As a final control for any possible effects of attention, we compared baseline spiking rates over the different off-durations. Attention has previously been shown to increase baseline spiking rates and fMRI BOLD signal in several extrastriate areas (Kastner et al. 1999; Luck et al. 1997; Williford and Maunsell 2006), but no such differences were apparent in our data (ANOVA, all $P > 0.54$). Whereas these analyses do not definitively eliminate the possibility of an influence of the animal's attentional state on our findings, the absence of any statistical differences does render it unlikely that attention played a crucial role in reducing response variability in our experiments.

While previous studies demonstrate that the mere presence of a stimulus reduces neuronal variability (Churchland et al. 2010) and that attended stimuli evoke responses with lower variability than unattended stimuli (Mitchell et al. 2007), our results demonstrate that stimulus-evoked variability reductions also crucially depend on the timing with which the driving stimuli are presented. This suggests that standard network-driven response stabilization is a time-consuming process that stabilizes the activity patterns of individual neurons more strongly when it is given more time to reorganize itself during the blank duration. Moreover, since all the basic effects we report in this study are seen with all three stimuli, neuronal response stabilization might be a generic cortical mechanism that facilitates the efficient encoding of repeated stimulus presentations by increasing the signal-to-noise ratio of the neural code. It would therefore be interesting to investigate the temporal evolution of response stabilization within the local cortical network by simultaneously recording the responses of many neurons while they are being stimulated with sequences of stimuli separated by systematically varied blank durations. The hypothesis of a network-driven reduction in response variability also predicts that the spontaneous activity preceding stimulus presentation should become more regular. Unfortunately, the spontaneous activity we recorded in the present study was of too low a magnitude to reliably test this prediction.

Perceptual stabilization. This neurophysiological study of the effect of interstimulus blank duration on neuronal response properties was inspired by the psychophysical phenomenon of perceptual stabilization (Klink et al. 2008; Leopold et al. 2002). Over the last few years, insightful results about the nature of perceptual stabilization have been obtained with

behavioral studies (Brascamp et al. 2008; Carter and Cavanagh 2007; Kanai et al. 2007; Klink et al. 2008, 2009; Knapen et al. 2009; Pastukhov and Braun 2008), neural imaging (Raemaekers et al. 2009), brain stimulation (Brascamp et al. 2010), and computational approaches (Gigante et al. 2009; Noest et al. 2007; Wilson 2007), but it currently remains unclear how the activity patterns of single neurons are altered when perception stabilizes. Obviously, our present study cannot directly provide an answer to this question. It does, however, allow some tentative speculation about the relationship between perceptual stabilization on the one hand and neuronal response stabilization on the other. For instance, it is generally believed that the brain's initial "choice" for one of the perceptual interpretations of an ambiguous stimulus depends on small random fluctuations in the activity patterns of the neurons that represent the competing percepts (Noest et al. 2007). Whereas response stabilization occurred for all our stimuli, not only the ambiguous one, a reduction of minor neuronal activity fluctuations around a delicate perceptual choice moment may have much more profound effects on perception than an equally large reduction of neuronal fluctuations in the firm representation of an unambiguous stimulus.

On this account, it is intriguing to note that the neuronal response stabilization demonstrated in our study similarly depends on off-durations as the perceptual stabilization that was previously demonstrated in behavioral experiments (Klink et al. 2008; Noest et al. 2007). Whereas current computational models can explain a wide range of experimental findings on perceptual stabilization (Pearson and Brascamp 2008), they do not yet contain enough detail to reproduce our measures of variability. However, in a prominent computational model of perceptual stabilization, the strength of stabilization can be manipulated with a crucial parameter (β) for which a decisive neurophysiological interpretation is currently lacking (Noest et al. 2007). Interpreted either as an intraneural baseline that interacts with the adaptation state or as the strength of connectivity between percept- and adaptation-state carrying neurons, such a parameter might very well depend on interactions within the local network. Taking these models to the next neurophysiologically plausible level would require the incorporation of two important factors that can be derived from our results. First, the indirect effect of response magnitude on neuronal stabilization could be an important nonlinearity in the system, potentially related to the biophysics behind the spike-generating mechanism. Second, the additional stabilizing effect of blank period duration, independent of response magnitude, may involve complex local network interactions and their, potentially subthreshold, effects on the neuronal dynamics.

ACKNOWLEDGMENTS

We thank André Noest for useful discussions and advice about data analysis, Jacob Duijnhouwer for assistance with the custom software, and Theo Stuivenberg, Hans Borgeld, Henk Westland, and Ed van der Veen for technical support. Bert van den Berg, Joost le Feber, and Naotsugu Tsuchiya commented on earlier versions of this manuscript.

GRANTS

Support for this work was provided by Netherlands Organisation for Scientific Research (VIDI; 016.001.026 and 051.14.027) and Utrecht University (High Potential; "Neural mechanisms of voluntary control") to R. J. A. van Wezel.

DISCLOSURES

No conflicts of interest, financial or otherwise, are declared by the author(s).

AUTHOR CONTRIBUTIONS

Author contributions: P.C.K., M.J.L., and R.J.A.v.W. conception and design of research; P.C.K. performed experiments; P.C.K. analyzed data; P.C.K., A.O., M.J.L., and R.J.A.v.W. interpreted results of experiments; P.C.K. prepared figures; P.C.K. drafted manuscript; P.C.K., A.O., M.J.L., and R.J.A.v.W. edited and revised manuscript; P.C.K., A.O., M.J.L., and R.J.A.v.W. approved final version of manuscript.

REFERENCES

Bair W, Koch C, Newsome W, Britten KH. Power spectrum analysis of bursting cells in area MT in the behaving monkey. *J Neurosci* 14: 2870–2892, 1994.

Belitski A, Gretton A, Magri C, Murayama Y, Montemurro MA, Logothetis NK, Panzeri S. Low-frequency local field potentials and spikes in primary visual cortex convey independent visual information. *J Neurosci* 28: 5696–5709, 2008.

Bokil H, Andrews P, Kulkarni JE, Mehta S, Mitra PP. Chronux: a platform for analyzing neural signals. *J Neurosci Methods* 192: 146–151, 2010.

Bradley DC, Chang G, Andersen RA. Encoding of three-dimensional structure-from-motion by primate area MT neurons. *Nature* 392: 714–717, 1998.

Brascamp JW, Kanai R, Walsh V, van Ee R. Human middle temporal cortex, perceptual bias, and perceptual memory for ambiguous three-dimensional motion. *J Neurosci* 30: 760–766, 2010.

Brascamp JW, Knapen TH, Kanai R, van Ee R, van den Berg AV. Flash suppression and flash facilitation in binocular rivalry. *J Vis* 7: 12.1–12, 2007.

Brascamp JW, Knapen TH, Kanai R, Noest AJ, van Ee R, van den Berg AV. Multi-timescale perceptual history resolves visual ambiguity. *PLoS One* 3: e1497, 2008.

Carter OL, Cavanagh P. Onset rivalry: brief presentation isolates an early independent phase of perceptual competition. *PLoS One* 2: e343, 2007.

Churchland MM, Yu BM, Cunningham JP, Sugrue LP, Cohen MR, Corrado GS, Newsome WT, Clark AM, Hosseini P, Scott BB, Bradley DC, Smith MA, Kohn A, Movshon JA, Armstrong KM, Moore T, Chang SW, Snyder LH, Lisberger SG, Priebe NJ, Finn IM, Ferster D, Ryu SI, Santhanam G, Sahani M, Shenoy KV. Stimulus onset quenches neural variability: a widespread cortical phenomenon. *Nat Neurosci* 13: 369–378, 2010.

Fontanini A, Katz DB. Behavioral states, network states, and sensory response variability. *J Neurophysiol* 100: 1160–1168, 2008.

Freeman ED, Driver J. Subjective appearance of ambiguous structure-from-motion can be driven by objective switches of a separate less ambiguous context. *Vision Res* 46: 4007–4023, 2006.

Fries P, Nikolić D, Singer W. The gamma cycle. *Trends Neurosci* 30: 309–316, 2007.

Galindo-Leon EE, Liu RC. Predicting stimulus-locked single unit spiking from cortical local field potentials. *J Comput Neurosci* 29: 581–597, 2010.

Gawne TJ. The local and non-local components of the local field potential in awake primate visual cortex. *J Comput Neurosci* 29: 615–623, 2010.

Gigante G, Mattia M, Braun J, del Giudice P. Bistable perception modeled as competing stochastic integrations at two levels. *PLoS Comput Biol* 5: e1000430, 2009.

Green DM, Swets JA. *Signal Detection Theory and Psychophysics*. New York: Wiley, 1966.

Grill-Spector K, Henson R, Martin A. Repetition and the brain: neural models of stimulus-specific effects. *Trends Cogn Sci* 10: 14–23, 2006.

Jacobs J, Kahana MJ, Ekstrom AD, Fried I. Brain oscillations control timing of single-neuron activity in humans. *J Neurosci* 27: 3839–3844, 2007.

Kaliukhovich DA, Vogels R. Stimulus repetition affects both strength and synchrony of macaque inferior temporal cortical activity. *J Neurophysiol* 107: 3509–3527, 2012.

Kanai R, Knapen TH, van Ee R, Verstraten FA. Disruption of implicit perceptual memory by intervening neutral stimuli. *Vision Res* 47: 2675–2683, 2007.

Kastner S, Pinsk MA, De Weerd P, Desimone R, Ungerleider LG. Increased activity in human visual cortex during directed attention in the absence of visual stimulation. *Neuron* 22: 751–761, 1999.

Katzner S, Nauhaus I, Benucci A, Bonin V, Ringach DL, Carandini M. Local origin of field potentials in visual cortex. *Neuron* 61: 35–41, 2009.

Kelly RC, Smith MA, Kass RE, Lee TS. Local field potentials indicate network state and account for neuronal response variability. *J Comput Neurosci* 29: 567–579, 2010.

Khayat PS, Niebergall R, Martinez-Trujillo JC. Frequency-dependent attentional modulation of local field potential signals in macaque area MT. *J Neurosci* 30: 7037–7048, 2010.

Klink PC, van Ee R, Nijs MM, Brouwer GJ, Noest AJ, van Wezel RJ. Early interactions between neuronal adaptation and voluntary control determine perceptual choices in bistable vision. *J Vis* 8: 16.1–16.18, 2008.

Klink PC, Noest AJ, Holten V, van den Berg AV, van Wezel RJ. Occlusion-related lateral connections stabilize kinetic depth stimuli through perceptual coupling. *J Vis* 9: 20.1–20.20, 2009.

Knapen T, Brascamp J, Adams WJ, Graf EW. The spatial scale of perceptual memory in ambiguous figure perception. *J Vis* 9: 16.1–16.12, 2009.

Kohn A. Visual adaptation: physiology, mechanisms, and functional benefits. *J Neurophysiol* 97: 3155–3164, 2007.

Kornmeier J, Ehm W, Bigalke H, Bach M. Discontinuous presentation of ambiguous figures: how interstimulus-interval durations affect reversal dynamics and ERPs. *Psychophysiology* 44: 552–560, 2007.

Kornmeier J, Hein CM, Bach M. Multistable perception: when bottom-up and top-down coincide. *Brain Cogn* 69: 138–147, 2009.

Leopold DA, Wilke M, Maier A, Logothetis NK. Stable perception of visually ambiguous patterns. *Nat Neurosci* 5: 605–609, 2002.

Liu J, Newsome WT. Local field potential in cortical area MT: stimulus tuning and behavioral correlations. *J Neurosci* 26: 7779–7790, 2006.

Logothetis NK. The underpinnings of the BOLD functional magnetic resonance imaging signal. *J Neurosci* 23: 3963–3971, 2003.

Luck SJ, Chelazzi L, Hillyard SA, Desimone R. Neural mechanisms of spatial selective attention in areas V1, V2, and V4 of macaque visual cortex. *J Neurophysiol* 77: 24–42, 1997.

Maier A, Wilke M, Logothetis NK, Leopold DA. Perception of temporally interleaved ambiguous patterns. *Curr Biol* 13: 1076–1085, 2003.

Maimon G, Assad JA. Beyond Poisson: increased spike-time regularity across primate parietal cortex. *Neuron* 62: 426–440, 2009.

Mayo JP, Sommer MA. Neuronal adaptation caused by sequential visual stimulation in the frontal eye field. *J Neurophysiol* 100: 1923–1935, 2008.

Mitchell JF, Stoner GR, Reynolds JH. Object-based attention determines dominance in binocular rivalry. *Nature* 429: 410–413, 2004.

Mitchell JF, Sundberg KA, Reynolds JH. Differential attention-dependent response modulation across cell classes in macaque visual area V4. *Neuron* 55: 131–141, 2007.

Mitra PP, Bokil H. *Observed Brain Dynamics*. New York: Oxford Univ. Press, 2007.

Mitra PP, Pesaran B. Analysis of dynamic brain imaging data. *Biophys J* 76: 691–708, 1999.

Murthy VN, Fetz EE. Synchronization of neurons during local field potential oscillations in sensorimotor cortex of awake monkeys. *J Neurophysiol* 76: 3968–3982, 1996.

Noest AJ, van Ee R, Nijs MM, van Wezel RJ. Percept-choice sequences driven by interrupted ambiguous stimuli: a low-level neural model. *J Vis* 7: 10.1–10.14, 2007.

Okun M, Naim A, Lampl I. The subthreshold relation between cortical local field potential and neuronal firing unveiled by intracellular recordings in awake rats. *J Neurosci* 30: 4440–4448, 2010.

Orbach J, Zucker E, Olson R. Reversibility of the Necker cube. VII. Reversal rate as a function of figure-on and figure-off duration. *Percept Mot Skills* 17: 615–618, 1966.

Parker A. Binocular depth perception and the cerebral cortex. *Nat Rev Neurosci* 8: 379–391, 2007.

Pastukhov A, Braun J. A short-term memory of multi-stable perception. *J Vis* 8: 1–14, 2008.

Pearson J, Brascamp JW. Sensory memory for ambiguous vision. *Trends Cogn Sci* 12: 334–341, 2008.

Raemaekers M, van der Schaaf ME, van Ee R, van Wezel RJ. Widespread fMRI activity differences between perceptual states in visual rivalry are correlated with differences in observer biases. *Brain Res* 1252: 161–171, 2009.

Sengpiel F, Blakemore C, Harrad R. Interocular suppression in the primary visual cortex: a possible neural basis of binocular rivalry. *Vision Res* 35: 179–195, 1995.

Sheinberg DL, Logothetis NK. The role of temporal cortical areas in perceptual organization. *Proc Natl Acad Sci USA* 94: 3408–3413, 1997.

Singer W, Gray CM. Visual feature integration and the temporal correlation hypothesis. *Annu Rev Neurosci* 18: 555–586, 1995.

Sussillo D, Abbott LF. Generating coherent patterns of activity from chaotic neural networks. *Neuron* 63: 544–557, 2009.

Victor JD, Goldberg DH, Gardner D. Dynamic programming algorithms for comparing multineuronal spike trains via cost-based metrics and alignments. *J Neurosci Methods* 161: 351–360, 2007.

Victor JD, Purpura KP. Nature and precision of temporal coding in visual cortex: a metric-space analysis. *J Neurophysiol* 76: 1310–1326, 1996.

Victor JD. Spike train metrics. *Curr Opin Neurobiol* 15: 585–592, 2005.

van Wezel RJ, Britten KH. Motion adaptation in area MT. *J Neurophysiol* 88: 3469–3476, 2002.

Williford T, Maunsell JH. Effects of spatial attention on contrast response functions in macaque area V4. *J Neurophysiol* 96: 40–54, 2006.

Wilson HR. Minimal physiological conditions for binocular rivalry and rivalry memory. *Vision Res* 47: 2741–2750, 2007.

Wolfe JM. Reversing ocular dominance and suppression in a single flash. *Vision Res* 24: 471–478, 1984.

Yao H, Shi L, Han F, Gao H, Dan Y. Rapid learning in cortical coding of visual scenes. *Nat Neurosci* 10: 772–778, 2007.

Zanos TP, Mineault PJ, Pack CC. Removal of spurious correlations between spikes and local field potentials. *J Neurophysiol* 105: 474–486, 2011.